Self-Diffusion in Binary Blends of Cyclic and Linear Polymers

Gopinath Subramanian[†] **and Sachin Shanbhag***[,†,‡]

Department of Scientific Computing, Florida State University, Tallahassee, Florida 32306-4120, and Department of Chemical and Biomedical Engineering, FAMU-FSU College of Engineering, Tallahassee, Florida 32310-6046

Received June 2, 2008; Revised Manuscript Received July 22, 2008

ABSTRACT: A lattice model is used to estimate the self-diffusivity of entangled cyclic and linear polymers in blends of varying compositions. To interpret simulation results, we suggest a minimal constraint release model for the motion of a cyclic polymer infiltrated by neighboring linear chains. Both the simulation and recently reported experimental data on entangled DNA solutions support the simple model over a wide range of blend compositions, concentrations, and molecular weights.

1. Introduction

According to classical theories of polymer physics, flexible chains in solution assume coiled conformations. As the polymer concentration or contour length is increased, these coils overlap and produce entanglement effects, which include a pronounced retardation of molecular mobility. For linear polymers (LP), this transition from unentangled to entangled dynamics is marked by a change in the zero-shear viscosity η_0 from $\eta_0 \sim M$ to $\eta_0 \sim M^{3.4}$ [1] and self-diffusivity D_L from $D_L \sim M^{-1}$ to $D_L \sim M^{-2.3}$,[2] where M is the molecular weight. The exact value of the exponent for D_L, while close to M^{-2}, is somewhat controversial and, for DNA solutions considered later in this paper, varies with concentration.[3,4] Molecular topology has a strong effect on the dynamics of polymers in the entangled state and constitutes a subject of fundamental and industrial interest in polymer physics and rheology. Although important gaps in understanding persist, the behavior of entangled linear and branched polymers, such as stars, are relatively well-described at small deformation rates, using the tube ansatz. Here, the molecular dynamics of a tracer chain enmeshed in a matrix of other molecules are formulated in terms of a diffusion problem that describes the motion of *chain ends* in a hypothetical tube.[5−7]

Concentrated solutions of ring or cyclic polymers (CP), which lack chain ends, are scientifically intriguing since they defy a simple description in terms of the tube model. While interest in CPs has recently been rekindled, the conformational and dynamic properties of CPs in gels and in melts have been studied theoretically,[8−11] computationally,[12−16] and experimentally[17−23] since the 1980s. Almost all the theoretical and computational studies have investigated the characteristics of pure CPs and LPs, while blends of CPs and LPs have escaped the same level of scrutiny.[15,24,25] These blend systems are important for two reasons: (i) most experimental data on pure CPs are, in fact, data on cyclic−linear blends (CLB), due to contamination or limitations of purification methods, and (ii) the dynamics of such CLBs are extraordinarily sensitive to the concentration of LPs, as demonstrated by the linear viscoelastic response of polystyrene CLBs[26,27] and self-diffusion studies of DNA solutions.[4,28] These studies indicate a dramatic change in the mobilty of CPs that is both unexpected and unexplained and might supply deep insights into entangled polymer dynamics.

In this paper, a lattice-based dynamic Monte Carlo method called the bond-fluctuation model (BFM) is used to monitor the trajectory of LPs and CPs in entangled CLBs. A minimal model is constructed to interpret the diffusivities obtained from the simulation. This approximate theory is able to reasonably explain recent experimental data on entangled DNA solutions.

2. Model and Methods

We use Shaffer's version of the BFM,[29,30] which has recently been applied to blends of CPs and LPs.[24,25] Since the model has been described in detail previously, only a brief summary presented here. Monomers or beads are placed on a simple cubic lattice. To generate an equilibrated CLB, we insert n_C nonconcatenated CPs and n_L LPs, each consisting of N monomers, on a 3D cubic lattice in a simulation box of size $L \times L \times L$. To simulate meltlike behavior, the total fractional occupancy of the lattice is maintained at $\phi = \phi_C + \phi_L = 0.5$, where $\phi_i = n_i N/L^3$ represents the fractional occupancy of CPs ($i = C$) and LPs ($i = L$). A trial move is attempted by displacing a randomly selected bead, belonging to either a CP or LP, by one lattice unit. It is accepted if it does not violate the excluded volume, chain connectivity, and chain uncrossability constraints. One Monte Carlo step (MCS) consists of $(n_L + n_C)N$ trial moves. Throughout this article, length is expressed in units of lattice spacing and time in MCS.

In this study, we considered two series of CLBs, viz. $N = 150$ and $N = 300$. We varied the composition of the blend from $\phi_C = 0.5$ to $\phi_C = 0.0$, corresponding to the range between pure CPs to pure LPs, respectively, as summarized in Table 1. The equilibration time for $N = 150$ varied from approximately 10^6 to 2.5×10^6 MCS and for $N = 300$ from 10^7 to 2.5×10^7 MCS, with larger values corresponding to larger ϕ_L. After equilibration, the duration of the simulation, τ_{sim} was picked to ensure that molecules had diffused at least two radii of gyration. During this period, we tracked the positions of the molecules by taking snapshots at periodic intervals. To determine the self-diffusivity, we calculated the mean-squared displacement of the center-of-mass of LPs and CPs separately via $g_3(t) = \langle(\mathbf{r}_{cm}(t+\tau) - \mathbf{r}_{cm}(\tau))^2\rangle$. Here, the average extends over molecules of a given topology (LP or CP), and τ is a dummy time variable. The diffusion constant D was calculated from the slope of the mean-squared displacement according to the relation $dg_3(t)/dt = 6D$.

3. Results

To estimate the diffusion constants, we performed linear regression analysis on the mean-squared displacement $g_3(t)$ in the interval $t = 0.15\tau_{sim} - 0.7\tau_{sim}$, where the function $g_3(t)$ was almost perfectly linear (see Appendix). Data on pure CPs and LPs were obtained from the literature.[14,29] Figure 1 shows the

* Corresponding author: phone 850.644.6548; e-mail sachins@scs.fsu.edu.
† Florida State University.
‡ FAMU-FSU College of Engineering.

10.1021/ma801232j CCC: $40.75
Published on Web 09/03/2008

Table 1. Description of the Systems Simulated[a]

ϕ_L	R_L	$[g_3(\tau_{sim})/R_L]^{1/2}$	R_C	$[g_3(\tau_{sim})/R_C]^{1/2}$
		$N = 150$		
0.500	7.95 ± 0.10			
0.479	8.21 ± 0.07	3.32	5.85 ± 0.16	4.09
0.458	8.10 ± 0.07	3.30	5.82 ± 0.11	3.63
0.438	8.19 ± 0.08	3.23	5.76 ± 0.10	3.65
0.375	7.99 ± 0.08	3.15	5.80 ± 0.07	4.37
0.313	8.02 ± 0.09	2.83	5.50 ± 0.05	3.97
0.250	8.21 ± 0.10	2.39	5.54 ± 0.05	3.43
0.188	8.16 ± 0.12	2.32	5.46 ± 0.04	3.90
0.125	8.15 ± 0.15	2.50	5.30 ± 0.03	4.59
0.063	8.01 ± 0.18	2.58	5.25 ± 0.03	5.57
0.042	8.04 ± 0.25	2.68	5.25 ± 0.03	5.81
0.021	8.33 ± 0.34	2.49	5.16 ± 0.03	6.32
0.000			5.09 ± 0.14	
		$N = 300$		
0.500	11.20± 0.17			
0.450	11.32 ± 0.15	3.00	8.60 ± 0.20	2.64
0.375	11.51 ± 0.18	2.89	8.71 ± 0.20	2.73
0.250	12.27 ± 0.25	2.68	8.10 ± 0.11	3.41
0.167	12.02 ± 0.29	2.50	7.50 ± 0.11	3.77
0.125	11.80 ± 0.31	2.40	7.32 ± 0.10	4.12
0.100	12.37 ± 0.33	2.70	7.24 ± 0.08	4.86
0.050	12.35 ± 0.55	2.75	7.10 ± 0.07	6.27
0.025	11.67 ± 0.56	2.79	6.96 ± 0.05	7.41
0.000			7.02 ± 0.06	

[a] Simulation box size $L_{box} = 60$, and total density $\phi_C + \phi_L = 0.5$. The radii of gyration R_L and R_C are reproduced from ref 24 for reference. The third and fifth columns show that the molecules have diffused at least 2 times their radius of gyration during the simulation.

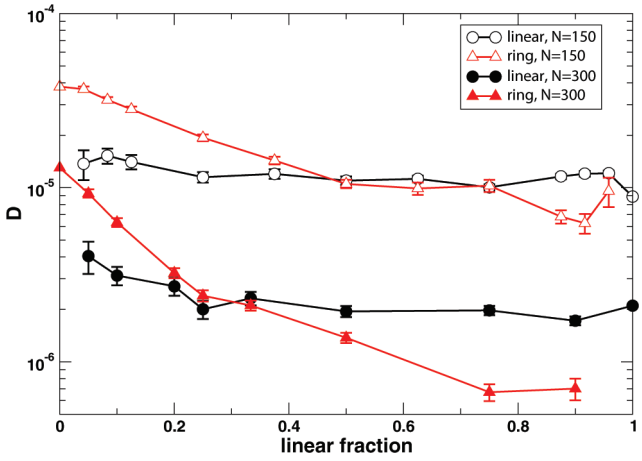

Figure 1. Self-diffusivity of the cyclic (triangles) and linear (circles) molecules for $N = 150$ (open symbols) and $N = 300$ (filled symbols) at different blend compositions.

variation of the diffusivity as a function of the fraction of the LPs for $N = 150$ and $N = 300$. As the linear fraction increases, the diffusivities of both the CPs and LPs decrease, although D_C drops more sharply. This is particularly evident for $N = 300$. Further, that decrease is most pronounced at small ϕ_L.

Experimental data on entangled DNA solutions (Figure 3 from ref 4) suggest that LPs diffuse more sluggishly in a LP matrix than in a CP matrix and that the strength of this slowdown increases with N. This is possibly the reason why the decrease in D_L at small ϕ_L is more prominent for $N = 300$. Other studies on polystyrene melts (Figure 2 from ref 22) suggest that D_L is independent of the composition of the blend, which appears to be true over a wide composition range in Figure 1. The apparent contradiction in these two data sets may be partially reconciled through our findings. In all likelihood, a small fraction of the supposed polystyrene CPs in the matrix were contaminated with LPs,[22] increasing the actual ϕ_L. It is then conceivable that in the window of observation the decrease in D_L at small ϕ_L was not captured.

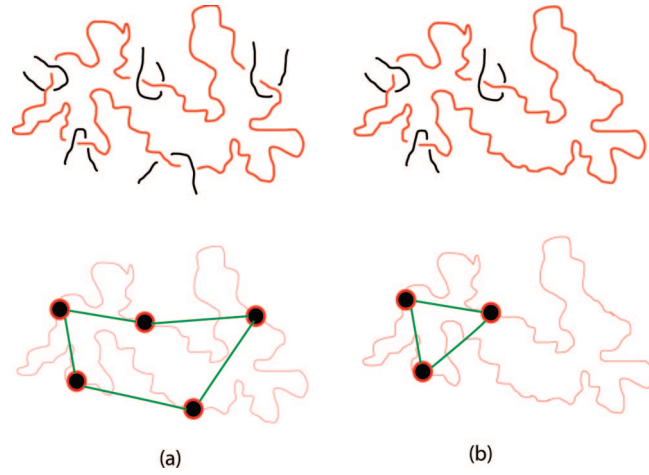

Figure 2. Number of entanglements on a CP Z_C depends on the concentration of LPs, ϕ_L. (a) and (b) correspond to large and small values of ϕ_L, respectively. Both Z_C (filled circles) and the length of the primitive path (green lines) of a CP of fixed molecular weight are proportional to ϕ_L, as depicted schematically by the figures at the bottom.[25] Each of these entanglements has a mean lifetime corresponding to the "reptation" time τ_L of the LP. In modeling the CR relaxation of the CP, we visualize the entanglements as Rouse beads with a frictional drag proportional to τ_L.

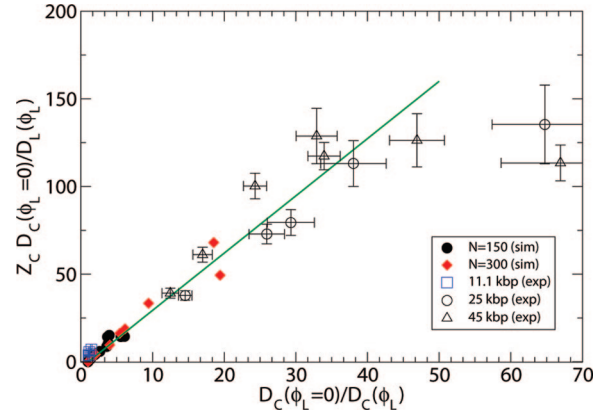

Figure 3. To validate eq 3, the self-diffusivity simulation data (solid symbols) on $N = 150$ (circles) and $N = 300$ (diamonds) and experimental data (open symbols) on the self-diffusivity of CPs in an entangled linear DNA matrix (ref 4) at different concentrations and three different molecular weights are replotted. The straight line confirms that there is a linear relationship between the quantities on the horizontal and vertical axes.

3.1. Minimal Model. Before we propose a framework to to interpret these simulation results, it is useful to recall pertinent findings from previous work on CLBs.[24,25] These investigations found that the radius of gyration of LPs was independent of blend composition, while CPs experienced modest swelling with increasing ϕ_L.[24] Primitive path analysis revealed that the average number of entanglements on a CP of a fixed molecular weight, Z_C, varied according to the linear fraction as $Z_C(\phi_L)/Z_L \sim \phi_L/\phi$, where $Z_L \approx N/30$ is the average number of entanglements on a LP which is independent of blend composition.[25] Similarly, the length of the primitive path of a CP, L_C, increased with increasing fraction of LPs according to $L_C(\phi_L)/L_L \sim \phi_L/\phi$, where the primitive path length of the LP L_L was also found to be independent of ϕ_L. This information, as it pertains to CPs, is portrayed schematically in Figure 2.

In the following minimal model, which ignores prefactors and other numerical details, we note that the threaded LPs

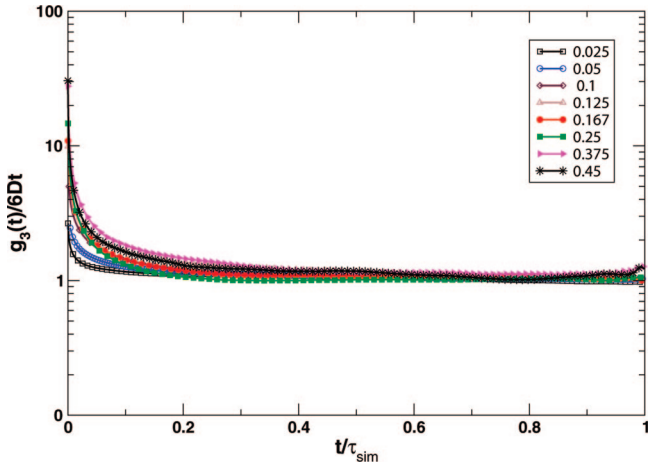

Figure 4. Ratio of $g_3(t)/6D_Ct$ for CPs with $N = 300$ approaches a plateau value of unity. The legend denotes the corresponding value of ϕ_L.

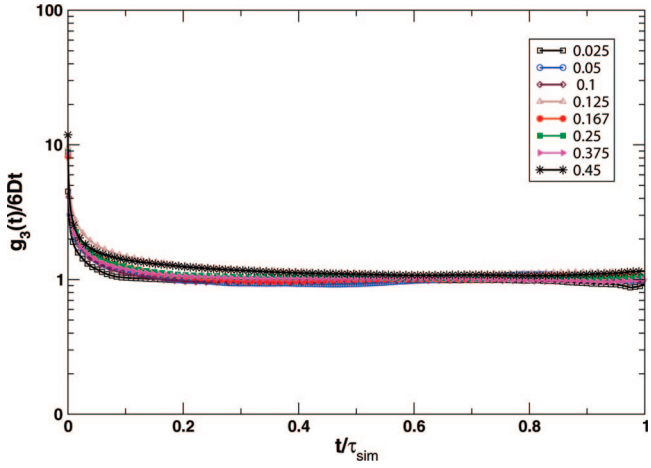

Figure 5. Ratio of $g_3(t)/6D_Lt$ for CPs with $N = 300$ approaches a plateau value of unity. The legend denotes the corresponding value of ϕ_L.

restrain the mobility of the CP. As some of the LPs venture out, others arrive and form entanglements at the same rate, and the equilibrium structure of the melt is not disturbed. Consequently, the primitive path of the CP itself undergoes local rearrangement as it relaxes by constraint release (CR) Rouse motion.[31] For a bidisperse or polydisperse blend of linear polymers the processes of reptation and CR occur simultaneously, as widely discussed in the literature,[31−37] and the faster process controls properties such as diffusivity and viscosity. A model based on a similar principle has also been proposed for the diffusion of CPs in a CLB.[38] In sharp contrast, on the basis of the physical picture described above, we hypothesize that the relaxation of a CP in a CLB is determined by the *slower* process. Under this premise, one can argue that

$$\frac{1}{D_C(\phi_L)} = \frac{1}{D_C(\phi_L = 0)} + \frac{1}{D_{CR}(\phi_L)} \tag{1}$$

where $D_C(\phi_L)$ and $D_C(\phi_L{=}0)$ are the diffusivities of a CP in a blend and in a pure melt (no LPs), respectively, and $D_{CR}(\phi_L)$ is the CR Rouse diffusivity, which will be specified shortly. When $\phi_L \approx 0$, it follows that $1/D_{CR} \approx 0$ and hence $D_C(\phi_L) \approx D_C(0)$. Similarly, when $Z_C \gg 1$, we expect $D_{CR}(\phi_L) \ll D_C(\phi_L = 0)$ and $D_C(\phi_L) \approx D_{CR}(\phi_L)$. Using standard CR arguments, the local hopping time for the Z_C "effective Rouse" beads (entanglements on the CP primitive path) is set by the LP relaxation time τ_L. The self-diffusivity of an ordinary N-bead Rouse chain is given by $D = k_BT/\zeta N$, where k_B is Boltzmann's constant, T is the absolute temperature, and ζ is the frictional drag per bead. If we assume that the effective drag on a CP in a CLB is dominated by entanglements with linear polymers and is proportional to $\tau_L = R_L^2(\phi_L)/D_L(\phi_L)$, we obtain $D_{CR}(\phi_L) \sim 1/\tau_L Z_C$. From previous simulations, $R_L(\phi_L)$ is independent of ϕ_L.[24,25] Thus, ignoring prefactors and constants, we get

$$\frac{1}{D_C(\phi_L)} = \frac{1}{D_C(\phi_L = 0)} + \frac{Z_C}{D_L(\phi_L)} \tag{2}$$

which can be rearranged to

$$Z_C\frac{D_C(\phi_L = 0)}{D_L(\phi_L)} = c_1\frac{D_C(\phi_L = 0)}{D_C(\phi_L)} + c_2 \tag{3}$$

where c_1 and c_2 are constants that account for terms neglected in this minimal model.

From our simulations (Figure 1) and from prior primitive path analysis,[25] all the parameters in eq 3 can be determined, and the viability of the minimal model can be ascertained. As shown in Figure 3, all the available simulation data, independent of composition and molecular weight, collapse on to a linear master curve (see Supporting Information).

To test whether experimental data may also abide by eq 3, we employed recently published self-diffusivity data on solutions of linear and cyclic DNA.[4] In this study, the authors used fluorescence microscopy to measure the diffusivities D_{ij} of tracer LPs and CPs, in a matrix of either LPs or CPs, where the subscripts i and j represent the topologies of the tracer and matrix molecules, respectively. These diffusivities were compiled as a function of contour length (5.9, 11.1, 25, and 45 kbp) and total solution concentration (up to 1 mg/mL), and for small values of these two variables the systems were not entangled. Using data on D_{LL} (linear tracer in a linear matrix), we demarcated the transition from unentangled to entangled dynamics. Thus, from Figures 2 and 3 in ref 4, we found that the 5.9 kbp sample is too short to be entangled, at any concentration. The concentrations at which the shift to reptation dynamics is observed for the pure LPs of length 11.1, 25, and 45 kbp samples was 0.7, 0.6, and 0.4 mg/mL, respectively.[39] For the most well-entangled systems, they observed $D_{CC} > D_{LC} > D_{LL} > D_{CL}$, which is in accordance with simulation data on $N = 300$. Thus, there are 16 data points available in the entangled regime at different lengths and concentrations for a tracer CP in a LP matrix. Under these conditions, $D_C(\phi_L) = D_{CL}$ and $\phi_L/\phi \rightarrow 1$. Similarly, $D_C(\phi_L = 0) = D_{CC}$ and $D_L(\phi_L) = D_{LL}$.

The total concentration c and contour length l contribute differently to the overall dynamics.[40] In the present analysis, the relevant relationships are the dependence of the average number of entanglements per chain on these two parameters. We recall that at a given c the average number of entanglements per polymer chain is proportional to its contour length, $Z_L \sim l$. Similarly, for a given l, the entanglement density increases with c. Since the modulus $G \sim c^{7/3}$ and the entanglement length $l_e \sim cRT/G \sim c^{-4/3}$, it follows that $Z_L \sim l/l_e \sim c^{4/3}$.[41] Thus, in the present case $Z_C = Z_L = (l/l_0)(c/c_0)^{4/3}$, where $l_0 = 3$ kbp and $c_0 = 1$ mg/mL were chosen,[4] although it should be pointed out that different values for the entanglement molecular weight of DNA solutions at $c_0 = 1$ mg/mL between $l_0 = 1$ and 30 kbp are supported in the literature,[42−44] although these latter data are more polydisperse and hence less reliable for the determination of l_0. If we superpose these data points (Figure 3), we find that although two of the 16 data points diverge from the trendline, the rest of the data are in very good agreement with the predicted linear dependence (see Supporting Information).

4. Summary

We performed Monte Carlo simulations to estimate the self-diffusivity of entangled CPs and LPs in blends and constructed

a simple constraint release model. Both the simulation and experimental data on entangled DNA solutions appear to obey the minimal model over a wide range compositions, concentrations, and molecular weights. The minimal model suggests that, unlike binary linear blends, the processes of constraint release and single molecule relaxation in cyclic−linear blends progress in series. Thus, analyses of these systems should help us to unravel some of the poorly understood aspects of the mechanism of constraint release.

Acknowledgment. We thank Doug Smith and Rae Robertson for sharing their data on entangled DNA and Ashish Lele, Balaji Iyer, Richard Graham, and Jorge Ramirez for helpful discussions. Partial support was provided by the Petroleum Research Foundation of the American Chemical Society through ACS PRF Grant 46770-G7 and the High-Performance Computing Center at Florida State University.

Supporting Information Available: Calculations for Figure 3. This material is available free of charge via the Internet at http://pubs.acs.org.

Appendix

The mean-squared center of mass, $g_3(t) = \langle(\mathbf{r}_{cm}(t+\tau) - \mathbf{r}_{cm}(\tau))^2\rangle$, becomes linear at long times. This may be ensured by monitoring the ratio $g_3(t)/6D_Ct$ (Figure 4, for $N = 300$) for CPs and $g_3(t)/6D_Lt$ (Figure 5, for $N = 300$) for LPs, which approaches a constant value of unity after a sufficiently long time. Similar profiles are observed for $N = 150$.

References and Notes

(1) Berry, G. C.; Fox, T. G. *Adv. Polym. Sci.* **1968**, *4*, 261–357.
(2) Lodge, T. P. *Phys. Rev. Lett.* **1999**, *83*, 3218–3221.
(3) Smith, D. E.; Perkins, T. T.; Chu, S. *Phys. Rev. Lett.* **1995**, *75*, 4146+.
(4) Robertson, R. M.; Smith, D. E. *Macromolecules* **2007**, *40*, 3373–3377.
(5) Doi, M.; Edwards, S. F. *The Theory of Polymer Dynamics*; Clarendon Press: Oxford, 1986.
(6) de Gennes, P. G. *Scaling Concepts in Polymer Physics*, 1st ed.; Cornell University Press: Ithaca, NY, 1979.
(7) Ball, R. C.; Mcleish, T. C. B. *Macromolecules* **1989**, *22*, 1911–1913.
(8) Cates, M. E.; Deutsch, J. M. *J. Phys. (Paris)* **1986**, *47*, 2121–2128.
(9) Rubinstein, M. *Phys. Rev. Lett.* **1986**, *57*, 3023–3026.
(10) Obukhov, S. P.; Rubinstein, M.; Duke, T. *Phys. Rev. Lett.* **1994**, *73*, 1263–1266.
(11) Iyer, B. V. S.; Lele, A. K.; Juvekar, V. A. *Phys. Rev. E* **2006**, *74*, 021805.
(12) Müller, M.; Wittmer, J. P.; Cates, M. E. *Phys. Rev. E* **1996**, *53*, 5063–5074.
(13) Müller, M.; Wittmer, J. P.; Barrat, J. L. *Europhys. Lett.* **2000**, *52*, 406–412.
(14) Brown, S.; Lenczycki, T.; Szamel, G. *Phys. Rev. E* **2001**, *63*, 052801.
(15) Geyler, S.; Pakula, T. *Makromol. Chem., Rapid Commun.* **1988**, *9*, 617–623.
(16) Hur, K.; Winkler, R. G.; Yoon, D. Y. *Macromolecules* **2006**, *39*, 3975–3977.
(17) Roovers, J. *Macromolecules* **1985**, *18*, 1359–1361.
(18) Roovers, J.; Toporowski, P. M. *J. Polym. Sci., Part B: Polym. Phys.* **1988**, *26*, 1251–1259.
(19) McKenna, G. B.; Hadziioannou, G.; Lutz, P.; Hild, G.; Strazielle, C.; Straupe, C.; Rempp, P.; Kovacs, A. J. *Macromolecules* **1987**, *20*, 498–512.
(20) McKenna, G. B.; Hostetter, B. J.; Hadjichristidis, N.; Fetters, L. J.; Plazek, D. J. *Macromolecules* **1989**, *22*, 1834–1852.
(21) Mills, P. J.; Mayer, J. W.; Kramer, E. J.; Hadziioannou, G.; Lutz, P.; Strazielle, C.; Rempp, P.; Kovacs, A. J. *Macromolecules* **1987**, *20*, 513–518.
(22) Tead, S. F.; Kramer, E. J.; Hadziioannou, G.; Antonietti, M.; Sillescu, H.; Lutz, P.; Strazielle, C. *Macromolecules* **1992**, *25*, 3942–3947.
(23) Semlyen, J. A. *Cyclic Polymers*, 2nd ed.; Springer: Dordrecht, The Netherlands, 2000.
(24) Iyer, B. V. S.; Lele, A. K.; Shanbhag, S. *Macromolecules* **2007**, *40*, 5995–6000.
(25) Subramanian, G.; Shanbhag, S. *Phys. Rev. E* **2008**, *77*, 11801.
(26) McKenna, G. B.; Plazek, D. J. *Polym. Commun.* **1986**, *27*, 304–306.
(27) Kapnistos, M.;Lang, M.;Rubinstein, M.;Roovers, J.;Chang, T.;Vlassopoulos, D. *Soc. Rheol. Annu. Meeting* **2006**.
(28) Robertson, R. M.; Smith, D. E. *Proc. Natl. Acad. Sci. U.S.A.* **2007**, *104*, 4824–4827.
(29) Shaffer, J. S. *J. Chem. Phys.* **1994**, *101*, 4205–4213.
(30) Shanbhag, S.; Larson, R. G. *Phys. Rev. Lett.* **2005**, *94* (7), 076001.
(31) Graessley, W. W. *Adv. Polym. Sci.* **1982**, *47*, 67–117.
(32) Rubinstein, M.; Colby, R. H. *J. Chem. Phys.* **1988**, *89*, 5291–5306.
(33) Viovy, J. L.; Rubinstein, M.; Colby, R. H. *Macromolecules* **1991**, *24*, 3587–3596.
(34) Green, P. F.; Mills, P. J.; Palmstrãm, C. J.; Mayer, J. W.; Kramer, E. J. *Phys. Rev. Lett.* **1984**, *53*, 2145–2148.
(35) Green, P. F.; Kramer, E. J. *Macromolecules* **1986**, *19*, 1108–1114.
(36) Graessley, W. W.; Struglinski, M. J. *Macromolecules* **1986**, *19*, 1754–1760.
(37) Liu, C. Y.; Keunings, R.; Bailly, C. *Phys. Rev. Lett.* **2006**, 97.
(38) Klein, J. *Macromolecules* **1986**, *19*, 105–118.
(39) The number of Kuhn segments in the 45 kbp sample is 150, since the Kuhn segment length is ∼300 bp. Similarly in the bond-fluctuation model, the number of Kuhn segments on the $N = 150$ sample is $0.83N = 125$.
(40) Rendell, R.; Ngai, K.; McKenna, G. *Macromolecules* **1987**, *20*, 2250–2256.
(41) Colby, R. H.; Rubinstein, M. *Macromolecules* **1990**, *23*, 2573–2757.
(42) Mason, T. G.; Dhople, A.; Wirtz, D. *Macromolecules* **1998**, *31*, 3600–3603.
(43) Goodman, A.; Tseng, Y.; Wirtz, D. *J. Mol. Biol.* **2002**, *323*, 199–215.
(44) Boukany, P. E.; Hu, Y. T.; Wang, S. Q. *Macromolecules* **2008**, *41*, 2644–2650.

MA801232J